한국공작기계기술학회 '96년도 춘계학술대회 논문집 pp 61~66

단섬유 금속복합체에서의 복합강화효과에 관한 연구

A Study on the Composite Strengthening Effect in Metal Matrix Composites

김홍건*, 전오성, 최창용
전주대학교 기계공학과

Hong Gun Kim*, Oh Sung Jun, Chang Yong Choi
Department of Mechanical Engineering, Jeonju University, Jeonju, Korea

Abstract

An overall feature to simulate composite behavior and to predict closed solution has been performed for the application to the stress analysis in a discontinuous composite solid. To obtain the internal field quantities of composite, the micromechanics analysis and finite element analysis (FEA) were implemented. For the numerical illustration, an aligned axisymmetric single fiber model has been employed to assess field quantities. Further, a micromechanics model to describe the elastic behavior of fiber or whisker reinforced metal matrix composites has been developed and the stress concentrations between reinforcements were investigated using the modified shear lag model with the comparison of finite element analysis (FEA). The rationale is based on the replacement of the matrix between fiber ends with the fictitious fiber to maintain the compatibility of displacement and traction. It was found that the new model gives a good agreement with FEA results in the small fiber aspect ratio regime as well as that in the large fiber aspect ratio regime.

It was found that the proposed simulation methodology for stress analysis is applicable to the complicated inhomogeneous solid for the investigation of micromechanical behavior.

1. Introduction

Composites, man-made material in which two or more constituents are combined to create a material with properties different from that of either constituent, have excited for thousands of years. The objective of fabricating composites is to improve mechanical preperties such as strength, stiffness, thoughness and high temperature performance. Therefore, it is natural to study together the composite that have a common strengthening mechanism. In composites in nature, loads are not directly applied on the fibers but are applied to the matrix material and transferred to the fibers through the fiber ends and also through the cylindrical surface of the fiber near the ends.

When the length of a fiber is much greater than the length over which the transfer of stress takes place, the end effects can be neglected and the fiber may be considered to be continuous.[1] In the case of short fiber composites, the end effects cannot be neglected and the composite properties are a function of fiber length. Furthermore, a significant stress concentration occurs between fibers.

Therefore, an correctly predictable appropriate theory is needed to evaluate the local and global properties for short fiber regime as well as long fiber regime. Early studies concerning variation of stresses along the length of a fiber were performed by Cox[2] and Outwater.[3] Probably the most often quoted theory of stress transfer is the shear lag (SL) analysis applied by Rosen,[4] who modified an earlier analysis of Dow.[5]

There have been limited previous attempts to modify the SL approach. Muki and Sternberg[6] and Sternberg and Muki[7] used the SL approach in a more refined manner using *integro-differential equations* and have calculated the local stresses inside the fiber.

However, this model assumed that the fiber center stress is given by the rule of mixture equation applicable strictly only to the long fiber case. Furthermore, Sternberg's results are not able to be applied to obtain expressions for the matrix stress intensification in the fiber end region which provides a significant contribution to the elastic modulus. On the other hand, Nardone and Prewo[8] and Nardone[9] attempted to modify the SL model by assuming that the fiber end stress was equal to the matrix yield stress and further that the matrix average stress was also equal to the matrix yield stress. This made possible an approximate estimate of the macroscopic composite yield strength increase, but this approach is clearly not applicable to the purely elastic regime wherein the elastic modulus increase is to be calculated. Taya and Arsenault[10] also attempted to modify the original SL approach by assuming that the fiber end stress was equal to the average matrix stress, i.e., the stress concentration at the fiber ends were ignored.

Recently, Kim and Nair[11] modified the SL analysis by using FEA to provide the fiber end normal stresses. Their results of the predicted internal stress and elastic modulus increases in short fiber reinforced MMCs showed a good agreement with FEA results as well as experimental data. While their work demonstrates that SL solutions have the applicability to the short fiber composite provided fiber end effects are accounted for, the model does not calculate the fiber end stresses from first principles and relies instead on FEA.

More recently, Kim[12] developed the SL closed form solution called MSL (Modified Shear Lag) model to provide the fiber end normal stresses. His approach involved replacing the matrix region between fiber ends with a fictitious fiber having the same elastic properties as the matrix and developing conventional SL solutions for both the *real* and *fictitious* fiber.

The purpose of this paper is to provide a rigorous evaluation of stress concentrations near discontinuity between fibers or whiskers using MSL model. An axisymmetric FEA model has been implemented to verify the predictions of the stress concentration effects. It was found that the MSL model is not only a correct prediction of the fiber stress increases in the small aspect ratio regime when compared to FEA results, but is also able to correctly predict the stress concentration effects in the matrix.

2. Modeling Procedure

Fig. 1 shows an overall procedure for composite analysis. From the given information, such as geometric and material properties, a designer can choose the analysis types and RVE depending on geometric and material characteristics. For an appropriate RVE, the boundary conditions should be considered rigorously. In the FEA preprocessing, it is quite efficient to set an coarse mesh in order to find out the correctness of overall results.

A micromechanical model is described as follows. The discontinuous short fibers are considered to be uniaxially aligned with the stress applied in the axial direction of the fibers. The fiber/matrix bond is assumed to be large and no debonding is allowed in keeping with the actual situation in many MMCs.[11] Further, no plastic yielding is allowed, that is, both matrix and fiber deform in a purely elastic manner. This rationale is an attempt to understand the initial stage of composite behavior. The conceptual approach of MSL model is shown in Fig. 1.

The conventional SL model is based on the concept that fiber tensile stresses are governed by an interfacial shear stress parallel to the fiber surface. In the MSL model, the short fibers are also considered to be uniaxially aligned with the stress applied in the axial direction of the fibers and the displacement and traction compatibility conditions are imposed to take the fiber end effect into account.

The micromechanical model to describe a short fiber reinforced composite is a single fiber model as shown in Fig. 2. In this model, a uniform fiber distribution with an end gap value equal to transverse spacing between fibers was selected. The fibers were assumed as uniaxially aligned with no fiber/ matrix debonding allowed for, in keeping with the actual situation in many MMCs (Arsenault and Pande, 1984).

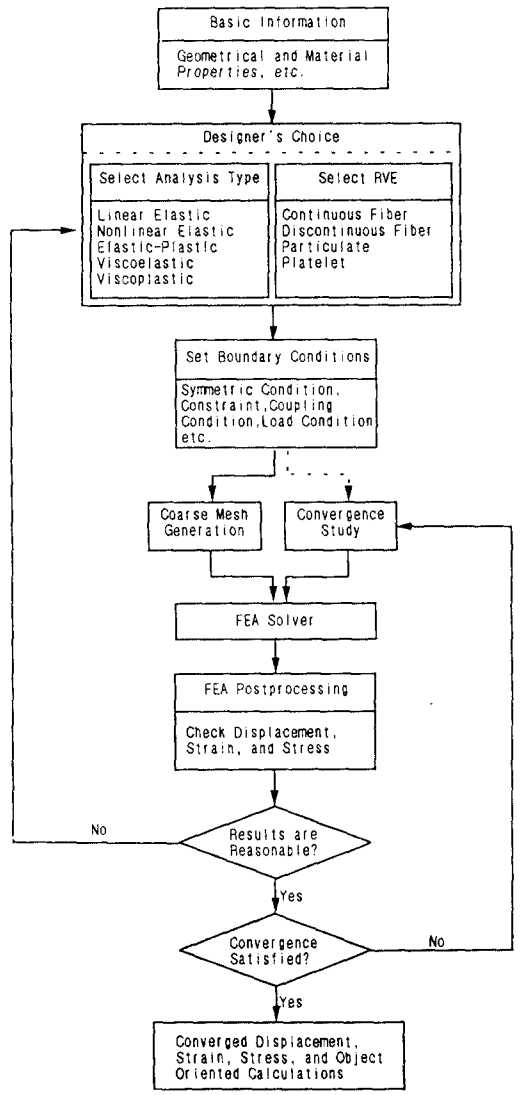

Figure 1 Overall computational Procedure for composite design.

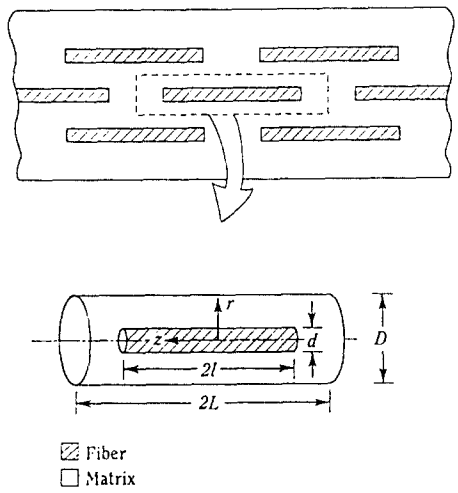

Figure 2 Composite RVE of a discontinuous composite

As shown in Fig. 3, the actual, or real, fiber has radius r, and length $2L$. On either end of the fiber is postulated a fictitious fiber also of diameter $2r$ but a length g=half the spacing between fiber ends in the composite. The outer surface of the unit cell can be said to have a hexagonal contour, however, the exact shape is not critical in this model. It is treated that the unit cell is an equivalent cylinder with radius R. The spatial variable for the real fiber is x, with the coordinate origin at the fiber center, whereas the spatial variable for the fictitious fiber is x^* with the coordinate origin at the fiber end.

In Fig. 3, different origins are necessary because, as to be shown, the governing differential equations in the region of the real and fictitious fiber are different and consequently there can be no overlap of the x and x^* domains. The two domains are in contact at x=L, or x^*=0, at which point proper boundary conditions need to be applied. Note, in the following, that all variables associated with the fictitious fiber will be denoted with a superscript *. At the far end of the unit cell, that is at the surface $x^*=g$, is applied a uniform constant composite strain ε_c.

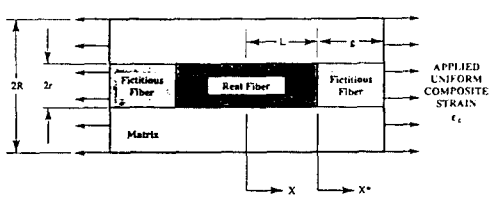

Fig. 3 The schematic of composite RVE containing fictitious whisker or fiber.

Through governing equations of the real and fictitious fiber, the solutions[12] are given by :

$$\sigma_f = E_f \varepsilon_c + A\sinh(nx/r) + B\cosh(nx/r) \quad (1)$$

$$\sigma_f^* = E_m \varepsilon_c + A^* \sinh(n^* x^*/r) + B^* \cosh(n^* x^*/r) \quad (2)$$

where

$$A = 0 \quad (3)$$

$$B = \frac{(E_m - E_f)\,\varepsilon_c}{\cosh(ns) + (n/n^*)\sinh(ns)\coth(n^* s^*)} \quad (4)$$

$$B^* = -B\,(n/n^*)\,\sinh(ns)\,\coth(n^* s^*) \quad (5)$$

$$A^* = -B^* \tanh(n^* s^*) \quad (6)$$

$$n^2 = \frac{E_m}{E_f\,(1+\nu_m)\,\ln(R/r)} \quad (7)$$

$$n^{*2} = \frac{1}{(1+\nu_m)\,\ln(R/r)} \quad (8)$$

Here, E_m and E_f are Young's moduli of the matrix and fiber, respectively, V_f is the volume fraction of fiber, ε_c is the far field composite strain and ν_m is the Poisson's ratio of the matrix. As mentioned above, R is the unit cell radius, s (=L/r) is fiber aspect ratio and s* (=g/r) is the aspect ratio of fictitious fiber.

Hence, the fiber maximum stress σ_{fm} can be obtained by setting x=0 in equation (1) :

$$\sigma_{fm} = E_f \varepsilon_c + B \quad (9)$$

In the same fashion, the fiber end stress σ_i can also be obtained by setting x^*=0 in equation (2), namely :

$$\sigma_i = E_m \varepsilon_c + B^* \quad (10)$$

Here, B^* can be described as a function of composite strain. Thus, we have

$$\sigma_i = (E_m + C)\,\varepsilon_c \quad (11)$$

where

$$C = \frac{(E_m - E_f)\,(n/n^*)\sinh(ns)\coth(n^* s^*)}{\cosh(ns) + (n/n^*)\sinh(ns)\coth(n^* s^*)} \quad (12)$$

Equation (11) represents that the interfacial stress is proportional to the composite strain as presumed. On the above basis, the stress concentration factor K_t can be calculated in the closed form as follows.

$$K_t = \frac{\sigma_i}{E_m \varepsilon_c} = 1 + \frac{C}{E_m} \quad (13)$$

On the other hand, FEA Model were generated for the verification of the present model. Fig. 4 describes the relevant meshes.

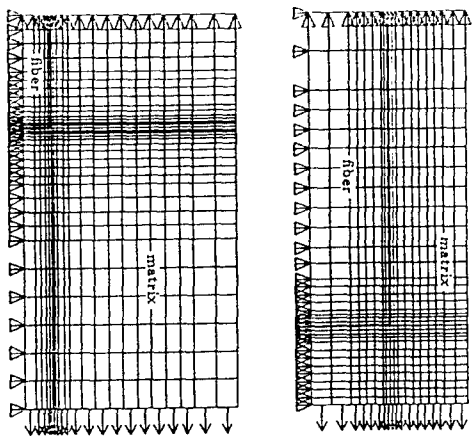

(a) (b)

Fig. 4 Axisymmetric FEA meshes of RVE at s=4 in case of (a) Quasi-infinite matrix (V_f = 0.5%) and (b) Finite Concentration (V_f = 20%).

3. Results and Discussion

Material properties selected are for Al 2124 as matrix and SiC whisker as reinforcement. For this system, typical values are E_m=67.2GPa, υ_m=0.33 for the matrix and E_f=480GPa, υ_f=0.17 for the fiber.[13,14]

The FEA computations were performed provided that the fiber or whisker distribution is perfectly uniform. The RVEs were selected for V_f=20% as well as V_f=0.5%. The configuration is similar to that used previously for a uniform distribution of fiber with an end gap value equal to transverse spacing between fibers.[15] In other words, g=R-r. For the side wall compatibility, the constraint conditions were imposed by requiring that the longitudinal cell boundary and the cell end are undistorted during deformation as implemented in the previous work.[16] The analytical result of the present model (MSL) is compared to the FEA results as well as to the prediction of the SL model.

The axial tensile stress in the fiber and matrix end region (fictitious fiber) at 0.1% composite strain is given in Fig. 5 for the case of a single fiber in a quasi-infinite matrix (V_f = 0.5%). For this case, r = 1, L = 4, g = 10, s = 4, s^* = 10, R/r = 7.56, n =0.2281, n^* = 0.6097. The analytical result of this model (MSL) is compared to the FEA results as well as to the prediction of the SL model. As shown in Fig. 5, the fiber stress in the SL model drops to zero as the fiber end region is approached. Further, the tensile stress in the matrix end region in the SL model is assumed constant throughout the gap region and equal to the average matrix stress (=$E_m\varepsilon_c$). On the other hand, in the MSL model the fiber stresses are significantly higher than that in the SL model. These fiber stresses drop off to a finite interfacial value σ_i at the fiber end. The tensile stress in the matrix end region is not constant but decreases from the value at the fiber and approached the SL model predictions at large distances from the fiber end. Further, note that the shape of the fiber tensile stress curve in the MSL model is not the same as that in the SL model because of the different constant values in the SL equation solutions.

For finite fiber concentrations (V_f = 20%), the results are shown in Fig. 6. Numerical values were set as r = 1, L = 4, g = 1, s = 4, s^* = 1, R/r = 2, n = 0.3897 and n^* = 1.0415. Note from Fig. 6, that the matrix stresses in the end gap region are throughout larger than the average matrix stress, predicted by the SL model. An interfacial value σ_i is also larger than that for the V_f = 0.005 case. Thus far, fiber end gap stresses and σ_i are increased as the fibers come close together along the axial direction.

The tensile results of the MSL model is in both qualitative and quantitative agreement with the FEA results, both for the single fiber (Fig. 5) and finite fiber concentration cases (Fig. 6). However, note that the maximum stress predicted at the fiber center by the MSL model in Fig. 6 is somewhat higher than the FEA result. This is due to the $\ln(R/r)$ term in equation (7) and (8). The SL and MSL model is clearly invalid as R→∞ and, in this sense, is similar to the equation for the line tension of dislocations in metallic alloys. At more realistic fiber concentrations, the FEA and MSL predictions are in better agreement as shown in Fig. 6. The MSL model is also not applicable in the limit as R→r, for, in this case, as equation (7) and equation (8) show, the fiber stresses show a singularity.

Interfacial shear stresses at 0.1% composite strain are depicted in Fig. 7 and Fig. 8 for V_f = 0.005 and V_f = 0.2, respectively. For the case of the single fiber in an quasi-infinite matrix (V_f = 0.005), Fig. 7 indicates that the trends in shear stress show good agreement

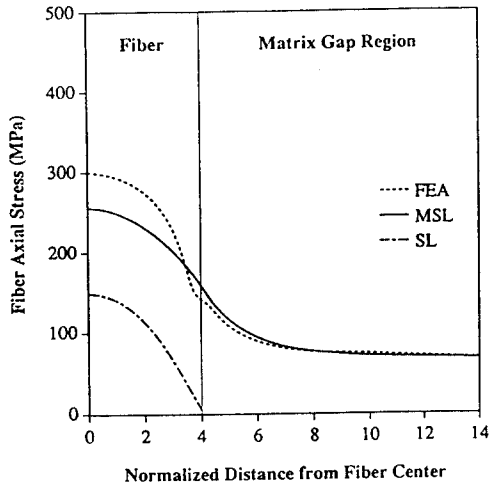

Fig. 5 Real and fictitious fiber axial stress distributions as predicted by SL, MSL and FEA at ε_c = 0.1% in case of V_f = 0.5%.

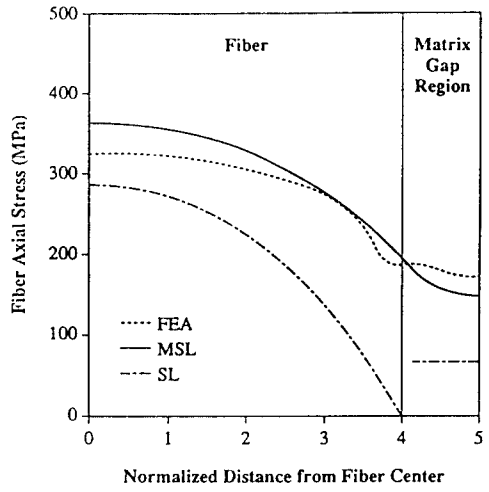

Fig. 6 Real and fictitious fiber axial stress distributions as predicted by SL, MSL and FEA at ε_c = 0.1% in case of V_f = 20%.

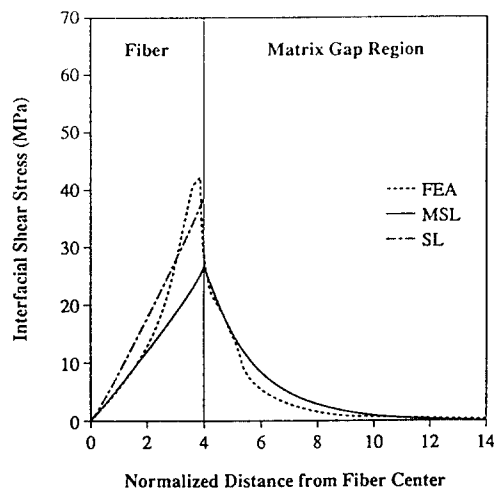

Fig. 7 Interfacial shear stress distributions as predicted by SL, MSL and FEA at ε_c=0.1% in case of V_f=0.5%.

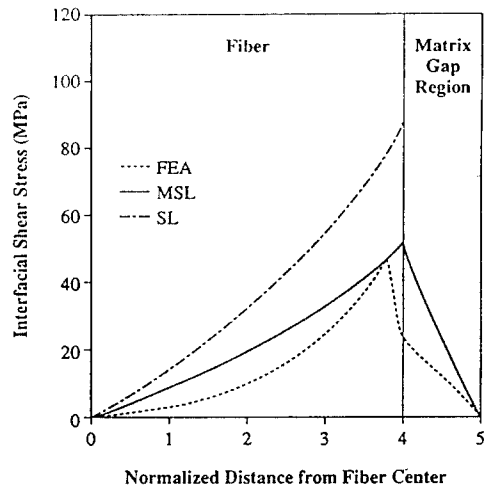

Fig. 8 Interfacial shear stress distributions as predicted by SL, MSL and FEA at ε_c=0.1% in case of V_f=20%.

between the MSL model and FEA predictions. Note, however, that the SL model does not provide any shear stress values in the end gap region. The shear stresses at the fiber/matrix interface near the fiber end is somewhat underestimated in the MSL model, again due to the $\ln(R/r)$ term as explained earlier. The predicted shear stresses in the gap region by the MSL model agree excellently with calculated FEA results. For the more realistic case of V_f = 0.2, Fig. 8, there is even better agreement between the FEA shear stress results and that of the MSL model over both the fiber/matrix interface and the matrix gap regions. If local plastic yielding is driven by a *Tresca* criterion, Fig. 7 and 8 predict that plasticity would progress both into the gap region from the fiber end due to the high shear stresses there as well as towards the fiber center from the fiber corners because of the high shear stresses at the fiber/matrix interfaces near the fiber end. Consequently, plastic yielding of the composite would commence at stresses lower than the macroscopic matrix yield stress. These shear stress values can then be used to estimate the approximate size of locally

yielded zones around the short fiber ends.

Again, MSL predictions agree well with FEA results. Accordingly, it is found that the present model can accurately describe the stress concentration factors, which is an important parameter to investigate the onset of yielding in the composite.

4. Conclusions

A simulation methodology for stress analysis was investigated to predict the internal quantities. It was found that the local deformation behavior in composite can be simulated depending on the designer's choice. The numerical examples show that the modified shear lag model can be implemented well to evaluate the stress concentration factors for the case of different modulus ratio and end gap size. Those match with FEA results in a good manner. It was found that the shear lag concept is also useful and simple enough to predict and stress concentration factors.

References

(1) Agarwal, B.D. and Broutman, L.J., 1980, "Analysis and Performance of Fiber Composites," John Wiley and Sons, New York, pp. 71-104.

(2) Cox, H.L., 1952, "The Elasticity and Strength of Paper and Other Fibrous Materials," British Journal of Applied Physics, Vol. 3, pp. 72-79.

(3) Outwater, J.O., 1956, "Modern Plastics," (March 1956), pp. 56.

(4) Rosen, B.W., 1964, "Mechanics of Composite Strengthening," in Fiber Composite Materials ASM, Metals Park, Ohio, 1964, Chapter 3.

(5) Dow, N.F., 1963, "Study of Stresses near a Discontinuity in a Filament-Reinforced Composite Material," General Electric Co. Report No. TISR63SD61.

(6) Muki, R. and Sternberg, E., 1969, "On the Diffusion of an Axial Load fron an Infinite Cylindrical Bar Embedded in an Elastic Medium," International Journal of Solids and Structures, Vol. 5, pp. 587-605.

(7) Sternberg, E. and Muki, R., 1970, "Load-Absorption by a Filament in Fiber Reinforced Material," Journal of Applied Mathematics and Physics (ZAMP), Vol. 21, pp. 552-569.

(8) Nardone, V.C. and Prewo, K.M., 1986, "On the Strength of Discontinuous Silicon Carbide Reinforced Aluminum Composites," Scripta Metallurgica, Vol. 20, pp. 43-48.

(9) Nardone, V.C., 1987, "Assessment of Models Used to Predict the Strength of Discontinuous Silicon Carbide Reinforced Aluminum Alloys," Scripta Metallurgica, Vol. 21, pp. 1313-1318.

(10) Taya, M. and Aresenault, R.J., 1989, "Metal Matrix Composites: Thermomechanical Behavior," Pergamon Press, pp. 25-28.

(11) Kim, H.G. and Nair,S.V., 1990, "Strengthening Analysis of SiC Whisker Reinforced Aluminum Alloys," Proceedings of the 11th World Korean Scientists and Engineers Conference, The Korean Federation of Science and Technology Societies, Seoul, Korea, June. 25-29, pp. 1737-1742.

(12) Kim, H.G., 1994, "Stress Transfer in Shear Deformable Discontinuous Composites," KSME Journal, Vol. 8, No. 4, pp. 475-484.

(13) Nair, S.V., Tien, J.K. and Bates, R.C., 1985, " SiC-Reinforced Aluminum Metal Matrix Composites," International Metals Review, Vol. 30, No.6, pp. 275-290.

(14) Nair, S.V. and Kim, H.G., 1991, "Thermal Residual Stress Effects on Constitutive Response of a Short Fiber or Whisker Reinforced Metal Matrix Composite," Scripta Metallurgica, Vol. 25, No. 10, pp. 2359-2364.

(15) Kim, H.G., 1994, "Assessment of Plastic Constraint Effects Induced by Whisker Interactions in Whisker Reinforced Metal Matrix Composites," Journal of Korean Society of Composite Materials, Vol. 7, No. 3, pp. 1-10.

(16) Kim, H.G., 1994, "A Numerical Study on the Evolution of Plasticity in a Heterogeneous Body," Journal of Basic Science Research Institute, Jeonju University, Vol. 7, No. 1, pp. 9-19.

(17) Nutt, S.R. and Needleman, A., 1987, "Void Nucleation at Fiber Ends in Al-SiC Composites," Scripta Metallurgica, Vol. 21, pp. 705-710.